www.elsevier.com/locate/matlet

Formation of anomalously large Al single crystals at triple points during pulsed electric current sintering (PECS) of $Al_{86}Ni_6Y_{4.5}Co_2La_{1.5}$ metallic glass

X.P. Li, J.Q. Wang, M. Yan, G. Ji, G.B. Schaffer, M. Qian

PII: S0167-577X(14)01123-9
DOI: http://dx.doi.org/10.1016/j.matlet.2014.06.077
Reference: MLBLUE17225

To appear in: *Materials Letters*

Received date: 13 May 2014
Accepted date: 12 June 2014

Cite this article as: X.P. Li, J.Q. Wang, M. Yan, G. Ji, G.B. Schaffer, M. Qian, Formation of anomalously large Al single crystals at triple points during pulsed electric current sintering (PECS) of $Al_{86}Ni_6Y_{4.5}Co_2La_{1.5}$ metallic glass, *Materials Letters*, http://dx.doi.org/10.1016/j.matlet.2014.06.077

Formation of anomalously large Al single crystals at triple points during pulsed electric current sintering (PECS) of $Al_{86}Ni_6Y_{4.5}Co_2La_{1.5}$ metallic glass

X.P. Li,[1,2,*] J.Q. Wang,[3] M. Yan,[1,4] G. Ji,[5] G.B. Schaffer,[1] and M. Qian[1,4]

[1]The University of Queensland, School of Mechanical and Mining Engineering, ARC Centre of Excellence for Design in Light Metals, Brisbane, QLD 4072, Australia

[2]The University of Western Australia, School of Mechanical and Chemical Engineering, Perth, WA 6009, Australia

[3]Shenyang National Laboratory for Materials Science, Institute of Metal Research, Chinese Academy of Sciences, Shenyang 110016, China

[4]RMIT University, School of Aerospace, Mechanical and Manufacturing Engineering, Melbourne, GPO Box 2476, VIC 3001, Australia

[5]Unité Matériaux et Transformations, UMR CNRS 8207, Bâtiment C6, Université Lille 1, 59655 Villeneuve d'Ascq, France

[*]Corresponding author email: xiaopeng.li@uwa.edu.au;

Abstract: Anomalously large aluminium single crystals with a size of ~ 500 nm have been observed at triple points between powder particles after pulsed electric current sintering below and in the supercooled liquid region in an $Al_{86}Ni_6Y_{4.5}Co_2La_{1.5}$ metallic glass. The formation of the large Al grains is attributed to high localized temperatures and the enhancement of long-range diffusion of Al by the electric current leading to grain growth and coalescence.

Keywords: Metallic glass; Diffusion; Pulsed electric current sintering; Crystallization

1. Introduction

To exploit the powder metallurgy approach for the fabrication of Al-based metallic glasses (MG), it is necessary to understand the thermal stability and the processes that occur during consolidation of the powder by sintering, including crystallization and grain growth. Given the challenges encountered in maintaining the amorphous structure, a variety of enhanced sintering techniques have been used, including pulsed electric current sintering (PECS). The PECS technique uses pressure and a pulsed electric current simultaneously. The process has a high thermal efficiency and materials densification by PECS is fast in most cases, thereby limiting grain growth. A key feature of PECS is the application of a current [1]. In addition to providing Joule heating, the current is also thought to affect mass transport in metals through the electron wind effect (electromigration) [2] and by a decrease in the activation energy for vacancy migration [3]. The combined effects lead to the enhancement of sintering.

We have previously reported on the PECS processing of fully amorphous $Al_{86}Ni_6Y_{4.5}Co_2La_{1.5}$ metallic glass powder [4, 5]. At heating rates of 40°C/min, clean sintered interfaces developed between two prior powder particles. It appeared that the surface oxide layer had been removed from these interfaces without triggering devitrification, which did not happen in the same material sintered at 5°C/min or when it was heated conventionally, where partial devitrification of the amorphous phase produced nanocrystalline Al grains (5-50 nm in size) [6]. We suggested in reference 4 that the high heating rates during PECS increased the electrical discharge at the two particle interfaces which assisted in the removal of the surface oxide layer, possibly through an evaporation-condensation mechanism [7]. Here, we re-examine the $Al_{86}Ni_6Y_{4.5}Co_2La_{1.5}$ material that had been consolidated by PECS at a heating rate of 40°C/min. In particular, we focus on the microstructure at triple point junctions and

report on the formation of anomalously large crystals of Al. Our observations suggest that the electric current may be the causal factor in the formation of these large crystals.

2. Materials and methods

Ingot samples with a nominal composition of $Al_{86}Ni_6Y_{4.5}Co_2La_{1.5}$ (in at. %) were prepared by arc melting high-purity elemental pieces of Al (>99.9 wt. %), Ni (>99.9 wt. %), Y (>99.0 wt. %), Co (>99.9 wt. %) and La (>99.0 wt. %) under a Ti-gettered argon atmosphere. Melting was carried out six times to ensure chemical homogeneity. The $Al_{86}Ni_6Y_{4.5}Co_2La_{1.5}$ powder was then produced by nitrogen-atomization of the ingots. The amorphous nature of the powder was examined using X-ray diffraction (XRD) and only powder particles smaller than 25 μm were used to ensure that they were fully amorphous. Powders were sintered using a SPS-1030 model (SPS SYNTEX INC, Japan). Based on our previous studies, the sintering temperatures were set to be 238.5, 248.5, 258.5 and 268.5°C, which lie below and in the supercooled liquid region (248.5 to 268.5°C) of the $Al_{86}Ni_6Y_{4.5}Co_2La_{1.5}$ alloy. The powder was placed into a tungsten carbide (WC) die and pressures of either 200 or 600 MPa were applied throughout the experiment. The heating rate was 40°C/min and samples were held at the sintering temperature for 10 minutes.

The microstructure after processing was characterized using an FEI Tecnai G2-20 Twin transmission electron microscope (TEM). The TEM samples were mechanically polished and then thinned by Precision Ion Polishing System (Gatan PIPS^{TM}) where low-angle and low-current polishing conditions were used in conjunction with a liquid nitrogen cold stage to avoid possible crystallization. A total of eight samples at different conditions (238.5, 248.5, 258.5, 268.5°C under 200 MPa and 238.5, 248.5, 258.5, 268.5°C under 600 MPa) were prepared. In each sample, the formation of large Al single crystals was observed. For convenience, only the sample sintered at 248.5°C and 600 MPa is discussed here.

3. Results and discussion

An area with three distinct regions is shown in the bright field TEM image in Fig. 1a. The broad halo diffraction ring in the selected area electron diffraction (SAED) pattern shown in Fig. 1b indicates an amorphous region, which is at the far left hand side of the image and may be the centre of particle P1. This would be the original, untransformed powder. The diffraction rings in Fig. 1c indicate that the surface regions of the prior particles labelled P1, 2 & 3 have partially crystallized into FCC Al nanocrystals with an average size of between 5 nm and 50 nm. Based on the precision electron micro diffraction patterns in Figs. 1d to f, a large Al crystal with a size about 500 nm is located in the triple junction area between three particles. Such large Al crystals were only found at triple junctions; no such big Al crystals were observed at the boundary between two neighboring particles. No other crystalline phases including complex intermetallic phases were detected.

TEM EDX line scan analysis, shown in Fig. 2a, indicates that the concentration of Al increases from the amorphous region to the large crystal region. However, the concentration of each of the alloying elements Ni, Y, Co and La first increases from the amorphous region towards the boundary with the Al nanocrystal region, then decreases towards the large Al crystal where it becomes zero. This is consistent with the EDX results shown in Fig. 2b. The concentration of Ni, Y, Co and La is similar on either side of the large Al crystal. This observation indicates that the influence of the sample thickness in this area on the EDX analyses can be neglected. However, the concentration variation of Al at triple points between powder particles is induced by diffusion which should show a gradual change. This is why the concentration of Al in the area close to the nanocrystal region is slightly lower than that in the center area of the large crystal region. The high resolution TEM (HRTEM) images in Figs. 3a and b further affirm the different microstructures of these two regions. The Al nanocrystal region is surrounded by amorphous matrix and defects are observable at the

boundary between the Al nanocrystal and the amorphous matrix whilst the large Al crystal is almost defect-free.

We have previously shown [6, 8] that the crystallization sequence for this alloy under conventional heating at a rate of 40°C/min starts at 282°C with the formation of FCC-Al crystals and is followed by the formation of a series of intermetallic phases at 289, 342 and 395°C. That no intermetallic phases were identified in the samples examined here suggests that the maximum temperature rise within the sample during PECS of $Al_{86}Ni_6Y_{4.5}Co_2La_{1.5}$ falls between 282 and 289°C. This is insufficient to melt the nanocrystals in the surface region of the particle. Together, these observations suggest that the large Al crystals in the triple junctions are unlikely to have formed by solidification, which is consistent with the microstructural observations. In addition, no obvious superplastic behavior was observed, although PECS was undertaken in the supercooled liquid region of the Al MG powder. A plasticity contribution to the formation of these large grains can therefore be neglected.

Others have observed a bimodal grain size in nanocrystalline material that had been processed by PECS [9-12]. This was brought about by grain growth and grain coalescence as a consequence of high localised temperatures and enhanced diffusion rates. It is possible that the large crystals we have observed at the triple points were also formed by grain growth and grain coalescence, which are diffusion controlled processes. That the local temperature does not seem to have been particularly high suggests that the diffusion kinetics have been enhanced.

The formation of nanocrystals in shear bands of an Al-rich MG has been attributed to an increase in the local mobility of Al atoms [13]. The origin of this enhanced atomic mobility was speculated to be the excess free volume in the shear bands which formed during deformation. This implies that diffusion, either short-range or medium-range, has an impact on thermal stability and the crystallization of MGs and that diffusion in MGs is affected by

the strain field. This was also addressed by a tracer measurement of enhanced atomic diffusion in a shear band of a Pd-based MG [14]. A weak static magnetic field is reported to suppress the diffusion of atoms in Al-rich glass forming alloy melts, which results in improvement of glass forming ability (GFA) [15]. The underlying reason was attributed to the Lorentz force generated from the magnetic field, which slowed down the atomic mobility. Based on the abovementioned research work, the diffusion of atoms in MGs is closely related to viscosity, relaxation, thermal stability and GFA. External fields including the electric field, the magnetic field and the stress field are expected to have an impact on the diffusion behavior in MGs [9-11].

Diffusion in metallic glasses has been debated for a long time [16-21]. Owing to the randomly packed structure of MGs without long-range order, it has been proposed that diffusion in MGs occurs by two distinct mechanisms at different temperatures [20, 22, 23]. At relatively high temperatures, i.e. in the supercooled liquid region, string-like cooperative diffusion behavior dominates. The diffusion of atoms with different radii is coupled and the relation between diffusion and viscosity and relaxation follows the Stokes-Einstein equation. When the temperature is below the experimentally determined glass transition temperature, i.e. in the glassy state, single atom hopping-like diffusion behavior takes effect. The diffusivity of small atoms is several orders of magnitude faster than that of mid-sized and large atoms. The diffusion of atoms with different radii is decoupled and the Stokes-Einstein relation no longer works [20, 21].

We speculate that the temperature at the surfaces of the particles at the triple points will be higher than elsewhere in the sample and will remain higher for longer, thus allowing more time for diffusion, which is boosted by electromigration [24] and enhanced defect mobility. More time for diffusion will in turn lead to further grain growth and coalescence and ultimately to anomalously large crystals at the triple points.

The uneven heat distribution across each powder particle is a consequence of the spatial distribution of the intensity of the electric discharge generated during PECS, which is related to the current input, the particle curvature, the distance between contacting particles and the shape of the contacting area [25]. The intensity of the electric field during PECS depends on the size, morphology and permittivity of the particles [26]. The spherical morphology of the powder particles and permittivity ratio between the powder and the air in the gap between the powders will enhance the electric field between neighboring particles [26], particularly in the triple points. This intensified electric field will ease the surface polarization relaxation process, which is related to trapping and detrapping of electrons from the surface [27]. More importantly, the surface polarization relaxation process will induce discharging or surface breakdown during PECS. As a result, more defects form, which in turn will accumulate more electron trapping and detrapping sites on the particle surface. This is why the Al nanocrystals form at the surface region of the MG powder, while the areas in the particle centers remain amorphous (Fig. 1a). Although this Joule heating is insufficient to melt the previously formed Al nanocrystals, the formation of these nanocrystals will result in more microstructural defects (Fig. 3a), which are also energy absorbing [28] and which will serve to further enhance the local temperature rise at the surface. This is supported by the observation that the nanocrystals are bigger (by about a factor of 10) in the vicinity of the triple point than they are adjacent to the amorphous region (Fig. 1a).

4. Conclusion

In summary, aluminium (Al) single crystals approximately 500 nm in size are observed between neighboring powder particles of an $Al_{86}Ni_6Y_{4.5}Co_2La_{1.5}$ metallic glass during pulsed electric current sintering. The formation of these large Al single crystals is attributed to the enhancement of long-range diffusion of Al atoms by the applied external electric field, leading to grain growth and coalescence.

This work was supported by the Australian Research Council (ARC) and the National Natural Science Foundation of China (No. 51131006). The authors gratefully acknowledge Dr. Hisashi Imai, Dr. Addad Ahmed and Dr. Tim Sercombe for the technical assistance and valuable discussion. X.L. acknowledges the financial support from the Graduate School International Travel Awards (GSITA), The University of Queensland (UQ), Unité Matériaux et Transformations (UMET, UMR CNRS 8207) at the Université de Lille 1, France and ECM Research Development Grant, the University of Western Australia (UWA).

References

[1] Munir ZA, Anselmi-Tamburini U, Ohyanagi M. J. Mater. Sci., 2006;41:763-77.

[2] Bertolino N, Garay J, Anselmi-Tamburini U, Munir ZA. Scripta Mater., 2001;44:737-42.

[3] Garay JE, Glade SC, Anselmi-Tamburini U, Asoka-Kumar P, Munir ZA. Appl. Phys. Lett., 2004;85:573-5.

[4] Li XP, Yan M, Imai H, Kondoh K, Schaffer GB, Qian M. J. Non-Cryst. Solids, 2013;375:95-8.

[5] Li XP, Yan M, Imai H, Kondoh K, Wang JQ, Schaffer GB, et al. Mater. Sci. Eng., A, 2013;568:155-9.

[6] Li XP, Yan M, Yang BJ, Wang JQ, Schaffer GB, Qian M. Mater. Sci. Eng., A, 2011;530:432-9.

[7] Toyofuku N, Kuramoto T, Imai T, Ohyanagi M, Munir Z. J. Mater. Sci., 2012;47:2201-5.

[8] Li XP, Yan M, Wang JQ, Huang H, Kong C, Schaffer GB, et al. J. Alloys Compd., 2012;530:127-31.

[9] Zhou F, Liao XZ, Zhu YT, Dallek S, Lavernia EJ. Acta Mater., 2003;51:2777-91.

[10] Zuniga A, Ajdelsztajn L, Lavernia EJ. Metall. Mater. Trans. A, 2006;37A:1343-52.

[11] Ye JC, Ajdelsztajn L, Schoenung JM. Metall. Mater. Trans. A, 2006;37A:2569-79.

[12] Kubota M, Wynne BP. Scripta Mater., 2007;57:719-22.

[13] Wilde G, Roesner H. Appl. Phys. Lett., 2011;98.

[14] Bokeloh J, Divinski SV, Reglitz G, Wilde G. Phys. Rev. Lett., 2011;107.

[15] Liu Z, Huang L, Huang B, Wei W, Chen Z, Huang Q, et al. Appl. Phys. Lett., 2012;100.

[16] Chen MW, Inoue A, Sakurai T, Menon ESK, Nagarajan R, Dutta I. Phys. Rev. B, 2005;71.

[17] Debenedetti PG, Stillinger FH. Nature. 2001;410:259-67.

[18] Iwashita T, Egami T. Phys. Rev. Lett., 2012;108.

[19] Tang XP, Geyer U, Busch R, Johnson WL, Wu Y. Nature. 1999;402:160-2.

[20] Yu HB, Samwer K, Wu Y, Wang WH. Phys. Rev. Lett., 2012;109.

[21] Zollmer V, Ratzke K, Faupel F, Meyer A. Phys. Rev. Lett., 2003;90.

[22] Loffler JF. Intermetallics. 2003;11:529-40.

[23] Wang WH, Dong C, Shek CH. Mater Sci Eng, R. 2004;44:45-89.

[24] Orchard HT, Greer AL. Appl Phys Lett. 2005;86:-.

[25] Munir ZA, Quach DV, Ohyanagi M. J. Am. Ceram. Soc., 2011;94:1-19.

[26] Chaim R. J. Mater. Sci., 2013;48:502-10.

[27] Legressus C, Blaise G. Ieee Transactions on Electrical Insulation. 1992;27:472-81.

[28] Kus M, Kenkre VM. Phys. Rev. B, 1992;45:9695-704.

Figure captions:

Fig. 1 (a) Bright field (BF) TEM image of a sample after FAS sintering of $Al_{86}Ni_6Y_{4.5}Co_2La_{1.5}$ MG powder particles, showing an amorphous region, a nanocrystal Al region and an Al single crystal. (b) and (c) are selected area electron diffraction (SAED) patterns from the amorphous region and nanocrystal Al region, respectively. (c) to (f) are precision electron micro diffraction patterns for the single crystal Al region. White dotted lines show the boundaries of three individual powder particles P1, P2 and P3. Insets are another two typical areas where Al single crystal form.

Fig. 2 (a) TEM EDX line scan along the red line in Fig. 1a across the entire region. Letter A, N and S represent the amorphous region, the nanocrystalline Al region and the single crystal Al region, respectively. LHS axis for Al and RHS axis for Ni, Y, Co and La. (b) TEM energy dispersive X-ray (EDX) point analysis on the single crystal Al region.

Fig. 3 (a) and (b) are high resolution TEM (HRTEM) images of the nanocrystal Al and single crystal Al regions, respectively. Red arrows show the defects and interfaces between the nanocrystal Al and surrounding amorphous matrix; black arrow and white arrow show the amorphous matrix and nanocrystal Al, respectively. Insets are fast Fourier transformation (FFT) patterns from the corresponding nanocrystal Al and single crystal Al region.

Highlights:

- Anomalously large Al single crystals form during PECS of Al-based metallic glass
- The size of the Al single crystals is around 500 nm
- The formation occurs at triple points between powder particles
- The underlying mechanism is the enhancement of long-range diffusion of Al
- Applied external electric field can influence diffusion in Al-based metallic glass

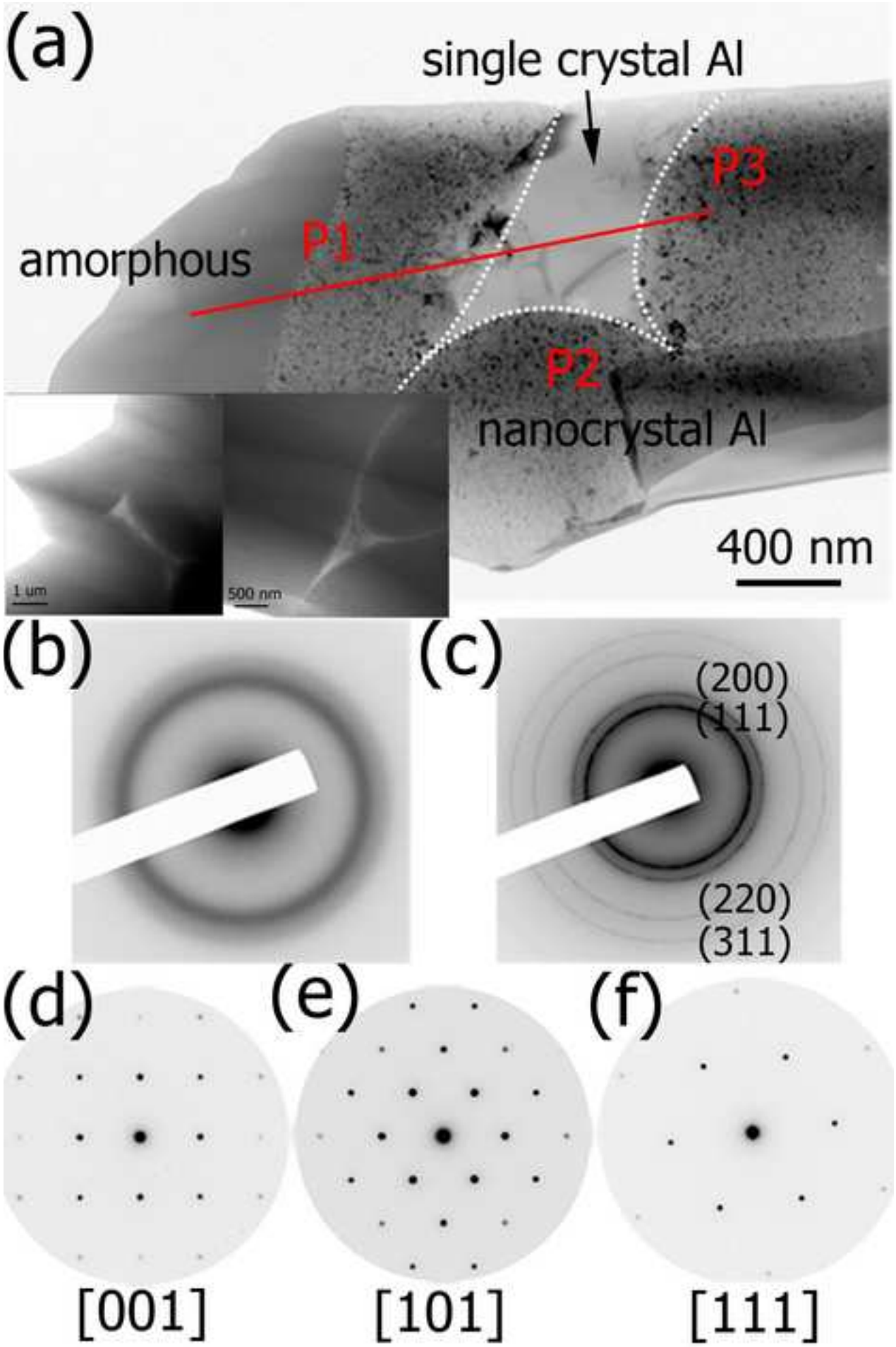

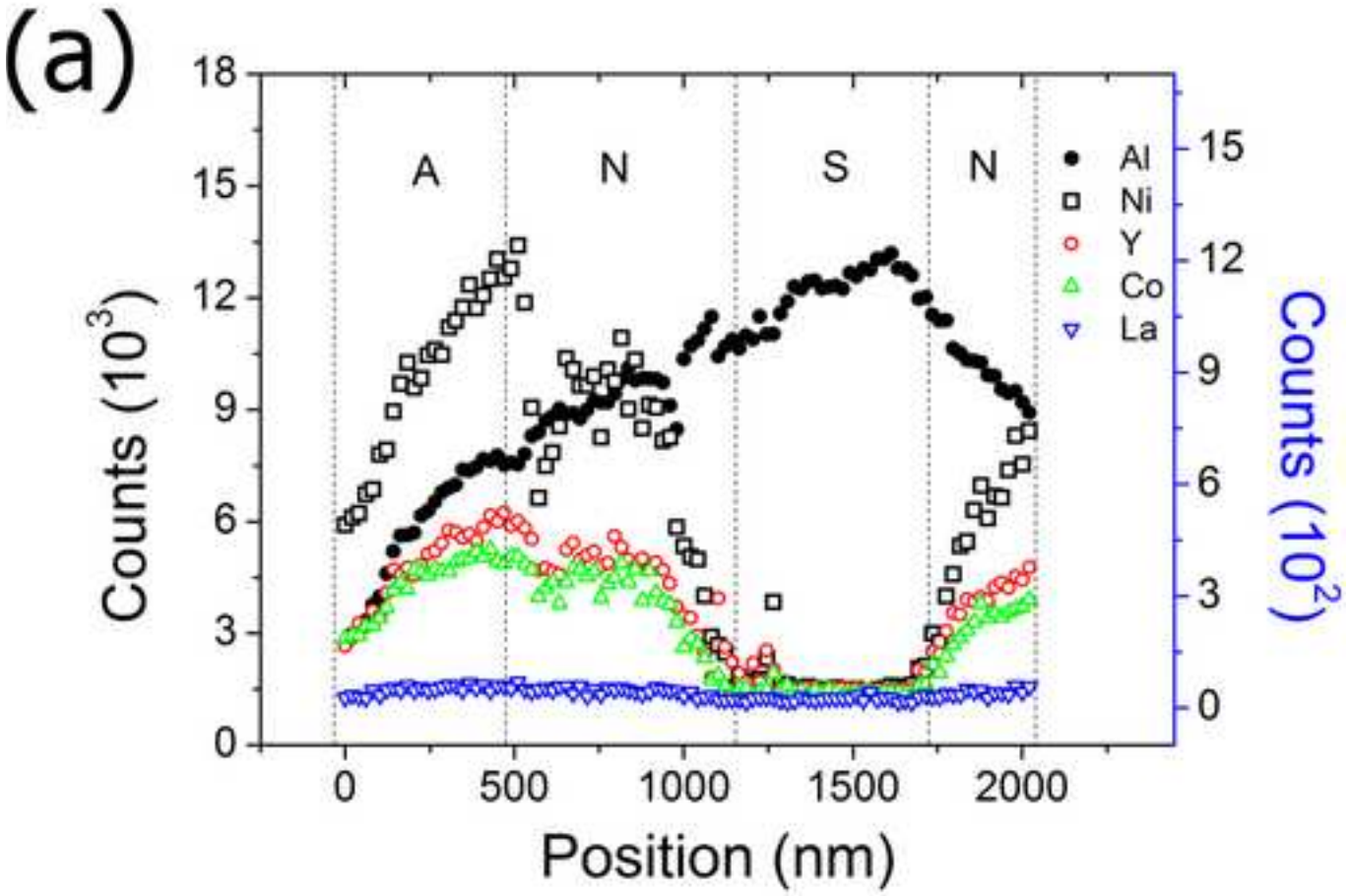

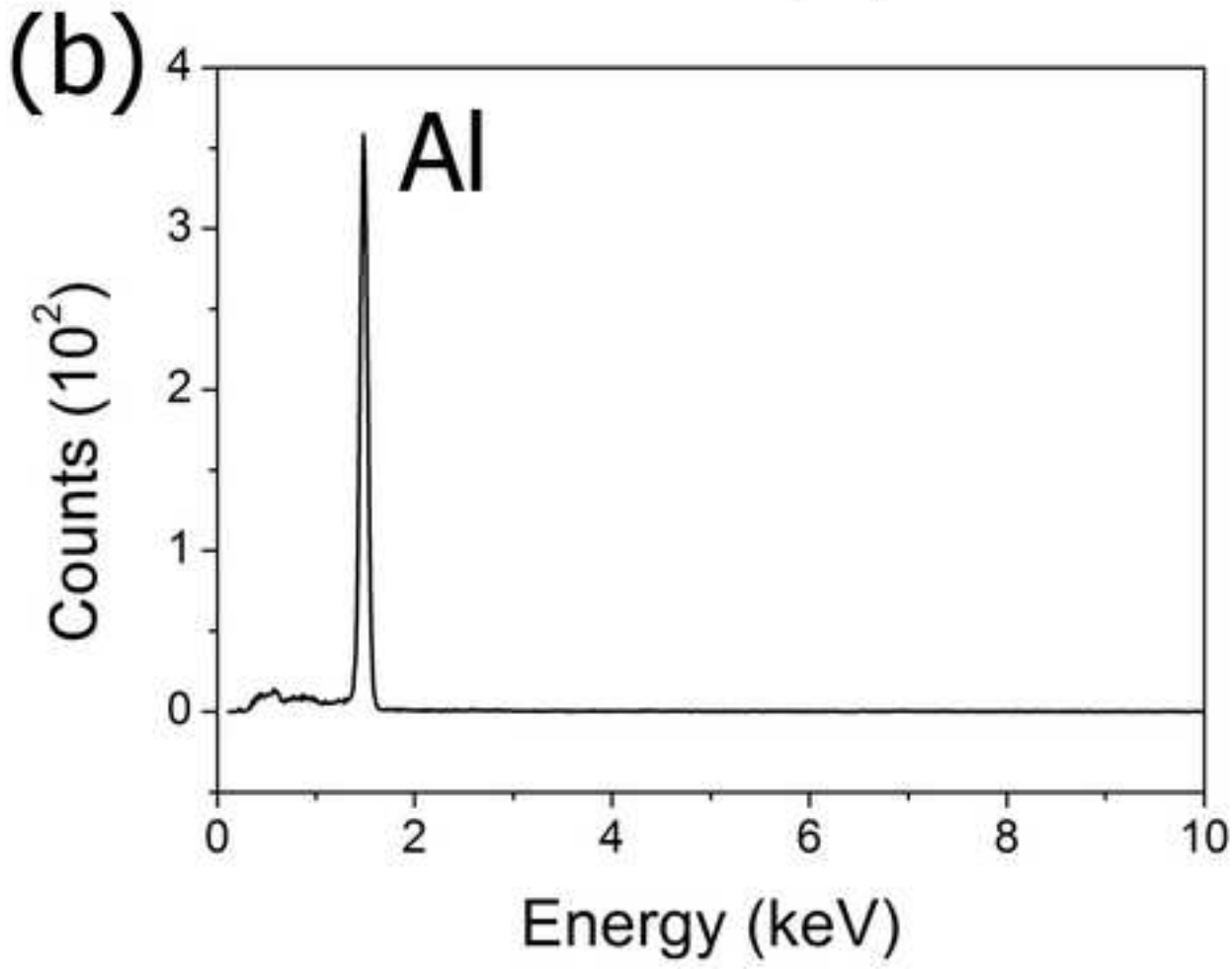

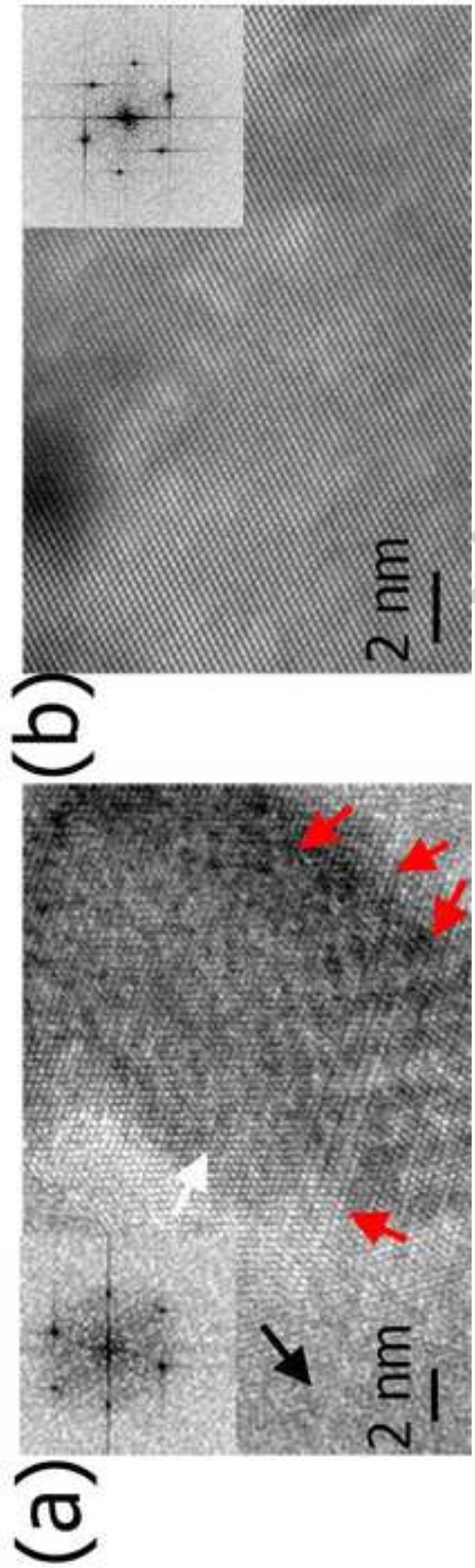

Figure